

UNIVERSIDADE DE SÃO PAULO

PUBLICAÇÕES

INSTITUTO DE FÍSICA
CAIXA POSTAL 20516
01498 - SÃO PAULO - SP
BRASIL

IFUSP/P-654

RESONANT HELICAL FIELDS IN TBR-1

I.L. Caldas, O.W. Bender, A.S. Fernandes, M.V.
A.P. Heller, M.Y. Kucinski, I.C. Nascimento,
I.H. Tan, A. Vannucci

Instituto de Física, Universidade de São Paulo



Agosto/1987

RESONANT HELICAL FIELDS IN TBR-1[‡]

I.L. Caldas*, O.W. Bender[†], A.S. Fernandes[‡], M.V.A.P. Heller,
M.Y. Kucinski, I.C. Nascimento, I.H. Tan, A. Vannucci

Instituto de Física, Universidade de São Paulo
C.P. 20516, 01498 São Paulo, S.P., Brazil

Abstract - The main characteristics of Mirnov oscillations, sawtooth oscillations and disruptions on the small brazilian tokamak TBR-1 are presented. The alteration of these characteristics caused by helical fields created by external resonant helical windings are also reported. Helical winding current thresholds for the destruction of the magnetic surfaces in TBR-1 caused by the interaction of different resonant fields are estimated. The radial dependence of the perturbations and the change in the shear over the island widths are taken into account. The toroidal corrections are discussed and the exact solution of the Laplace's equation for the magnetic scalar potential due to toroidal helical currents is presented.

1. INTRODUCTION

After the work on the Pulsator^[1], resonant helical windings have been used in other tokamaks to generate helical perturbations. Experiments with these external coils showed that macroscopic oscillations could be controlled and the nature of the disruptive instability could be investigated^[2,3].

In this paper we report some experimental and theoretical investigations which have been done on resonant helical fields in order to interpret and improve the plasma confinement in the tokamak TBR-1.

A short description of the TBR-1 and of the main experimental results obtained with this tokamak can be found in Ref. 4.

2. MACROSCOPIC OSCILLATIONS

Investigations of Mirnov oscillations, sawtooth oscillations and disruptions have been made on the TBR-1 device by using magnetic

probes, internal coils^[5] and soft x-rays^[6] diagnostics.

For the investigated discharges, the toroidal magnetic field was (0,37-0,45) T, the plasma current (6-13) kA, the mean electron density $\sim 5 \times 10^{18} \text{ m}^{-3}$ and the central electron temperature about 200 eV. The equilibrium was maintained by an externally applied vertical field. Without feedback control of the plasma position, equilibrium was obtained when the plasma column was displaced to the outside and to the bottom of the tokamak as indicated by the horizontal and vertical position coils^[7] and by the shape of the plasma boundary^[8].

Low-frequency magnetic oscillations were observed after the equilibrium state was set up. They were measured by 16 coils equally spaced in the poloidal direction at a fixed position and four coils separated 90° in the toroidal direction at a fixed poloidal position^[5]. The coils signals were recorded in two eight-channel ADC modules, and the usual phase correlation method was used to analyse the data.

Fig. 1 is a plot of the typical dependence of the Mirnov oscillation amplitudes on the poloidal position of the coils^[5]. The ratio $\bar{B}_\theta_{\text{max}}/\bar{B}_\theta_{\text{min}}$ is in general around 6. This asymmetry indicates that the magnetic islands which created the measured perturbations were, as so the entire plasma column, displaced downwards to the outside of the geometrical axis of the torus.

The investigated discharges can be characterized, in terms of the MHD activity, according the q_L (the safety factor at the limiter) values.

The discharges with higher q_L , which were sustained for $\lesssim 7$ ms, exhibit lower MHD activity that ceased after (2-3) ms, when hard x-rays signals (measured with an NaI crystal coupled to a photomultiplier and an active integrator) showed the appearance of runaway electrons. The discharges with smaller q_L had a much stronger MHD activity and a shorter duration. The modes grew, rotated and saturated at levels of $\bar{B}_\theta/\bar{B}_\theta$ of about 2%, which gave rise to magnetic islands with widths of about (1-2) cm for $m=2$ or 3.

The fluctuation amplitude was the only oscillation parameter noticeably dependent on q_L . The main detected modes had poloidal

*Partially supported by CNPq.

[†]Setor de Ciências Exatas, UFP, Curitiba, Brazil.

[‡]Instituto de Pesquisas Tecnológicas, São Paulo, Brazil.

[‡]Presented at the Energy Independence Conference/Fusion Energy and Plasma Physics (Rio de Janeiro, 1987).

numbers $m=2$ and $m=3$, always with $n=1$. Modes with $m=4$ are occasionally detected during high q_L discharges. The oscillation frequencies varied in time and were between 10 and 60 kHz. The modes rotated in the direction of the electron diamagnetic drift.

Sawtooth oscillations were also observed in several TBR-1 discharges through surface barrier detectors (Ortec Rg-019-50-100) that are sensitive to soft x-rays in the photon energy range between 0,1 and 30 keV. Five detectors were used in a pin-hole camera viewing the plasma volume.

Typical soft x-rays signals obtained for a $q_L = 3,2$ discharge are shown in Fig. 2^[6]. The sawtooth period was (100-150) μs and this oscillation had a modulation superimposed on it with a frequency of 50 kHz. This modulation was identified, by placing two x-rays detectors which are viewing two different positions 180° apart in the poloidal directions, as an $m=1$. The inversion of the sawtooth oscillation was used to estimate the $q=1$ surface localization.

3. RESONANT HELICAL WINDINGS

Resonant helical windings (rhw) were used to generate helical perturbations on TBR-1. Experiments with external m/n ($m=2, 3, 4$ and $n=1$) coils showed attenuation of the MHD activity for values of the helical currents such that $I/I_p \sim 2\%$ and also for two different pulse shapes.

As mentioned before, the equilibrium was maintained by an externally applied vertical field without feedback control of the plasma position. Thus, before discharge termination, the plasma column moved inwards. This displacement was usually anticipated when the coils were activated (see Fig. 3)^[9].

The experimental results obtained with $m=3$ coil current of 185 A (with radius $b=0.11$ m) are showed in Fig. 3^[9]. In this case the coil was activated .3ms before the beginning of the plasma discharge. The main noticeable effect of the coil was to reduce MHD activity mainly in the first 1.5 ms before the inward displacement of the plasma column started. Besides the dominant $m=3$ a sideband $m=2$ mode was also reduced

(the $m=3$ coil had also a secondary $m=2$ component).

The oscillation frequency increased with the coil activation and the consequent oscillation amplitude reduction (Fig. 4)^[9]. This agrees with the Mirnov oscillation property observed in Text^[10].

The effect of a $m=2$ rhw connected to a power supply which gives a square wave-like current pulse is shown in the Fig. 5^[6]. The coil was activated (during 0.8ms) 0.4ms after the plasma discharge was initiated. After the helical coil pulse ended the Mirnov oscillations increased again and some changes in the sawtooth parameters were observed.

4. MAGNETIC SURFACE BREAK-UP

We supposed that the magnetic surface break-up, caused by the interaction of magnetic islands with the limiter or the overlapping of magnetic islands, triggers the disruptions observed in TBR-1. We considered islands created by external windings and by helical surface currents on rational magnetic surfaces. The magnitude of these surface currents were obtained from experimental measurements of the poloidal magnetic field oscillations.

Applying the Chirikov's condition^[11], we estimated helical winding current thresholds for the break-up of the magnetic surfaces. We calculated these thresholds taking into account the r -dependence of equilibrium and perturbed magnetic fields over the islands widths.

To calculate the size of the islands we considered the large aspect-ratio approximation to obtain the magnetic surfaces from the differential equation

$$\vec{B} \cdot \nabla \psi = 0, \quad (1)$$

where ψ is the stream function corresponding to a linear superposition of the unperturbed fields described by $\psi_0(r)$ with the resonant perturbation described by $\psi_1(r,u)$, where $u = \theta - \alpha z$ and $\alpha = n/(mR)$. This approximation is not valid for marginally stable states when the plasma response should not be neglected.

ψ_1 was related to the perturbations created by currents I flowing (with opposite directions in adjacent conductors) in m pairs

of helical windings, equally spaced, with radius b ^[12]. ψ_1 could also correspond to saturated tearing perturbations due to a resonant helical current sheet.

These resonances create m magnetic islands around the rational surfaces with $q(r_{m,n}) = m/n$.

We consider also satellite magnetic islands due to toroidal corrections. To calculate the size of these ($m \pm 1$) satellite islands around the surfaces with $q(r_{m \pm 1, n}) = (m \pm 1/n)$, the magnetic differential equation (1) was solved by expanding it in terms of the aspect-ratio parameter and keeping terms which are resonant at the appropriate surface. Thus considering an m/n perturbation, we found a function X satisfying

$$\vec{B} \cdot \nabla X = 0, \quad (2)$$

near the surfaces with $q = m \pm 1$.

X was used in the same manner as ψ to apply Chirikov's condition and to obtain the helical current thresholds, taken into account the r -dependence of equilibrium and perturbed fields over the islands widths.

Examples of winding currents I required for the magnetic surface break-up (estimated considering the superposition of magnetic islands) are given in Fig. 6^[13].

In addition to the mentioned calculation based upon the overlap of magnetic islands, numerical work has been performed. The differential equations for the magnetic field lines have been integrated numerically for various perturbation strengths. Fig. 7 shows the intersection of the magnetic field trajectories with a poloidal plane $\varphi = 0$ for an equilibrium with $q(a) = 5$ and $q(0) = 1$ perturbed by a $m=2$ tearing mode with $\vec{B}_0/B_0 = 0.5\%$ and a $m=3$ helical current $I = 100$ A. In this figure it can be observed only a small amount of stochastic behaviour near the x -points of the islands although the application of the Chirikov's condition leads to the break-up of the magnetic surfaces. Thus, as expected from general mapping methods, this criterium underestimates the strength threshold for the relevance of the line chaotic distribution.

5. TOROIDAL HELICAL FIELDS

Magnetic scalar potential due to toroidal helical currents were calculated^[14] in order to investigate the influence of toroidal effects on the break-up of the magnetic surfaces.

The field due to a number of thin conductors wound on a circular torus carrying electrical currents was determined by solving Laplace's equation for the magnetic scalar potential using the conventional toroidal coordinates. The toroidal helical winding was characterized by the major and minor radii of the torus R_0 and b , respectively, by the number of periods of the helical field in the poloidal and toroidal directions m_0 and n_0 and by the winding law

$$m_0 \omega + n_0 \varphi = \text{constant}, \quad (3)$$

where ω and φ are toroidal coordinates^[14]. The exact solution was written as an infinite series of functions. Each term is of the order of a power of the inverse aspect-ratio (b/R_0).

In current papers^[12,15,16] approximate analytical expressions for the toroidal helical field are obtained considering helically symmetric systems bent into a torus. Approximate Laplace's equation for the scalar magnetic potential is written in terms of a local polar coordinate system.

Our approach has some advantages over the other one. (i) The boundary conditions for the approximate solutions of approximate Laplace's equation outside the torus are not clear. The problem is complicated by the fact that the effect of the winding law is as important as the other toroidal effects. Using the exact solution, different effects can be studied separately. (ii) The expression in terms of local polar coordinates cannot be used if scalelength of the order of b^2/R_0 is considered. So, the position of the magnetic axis, for example, cannot be determined. The expression in terms of toroidal coordinates does not present this problem.

The expressions obtained can be adapted without much difficulty to the case of a non-uniform winding law.

The results were compared to the ones obtained by solving the

approximate Laplace's equation^[14]. Both results coincide near the winding surface in some cases. However, outside the winding region, the results may differ significantly.

6. CONCLUSIONS

The main characteristics of Mirnov oscillations, sawtooth oscillations and disruptive instabilities on the tokamak TBR-1 have been determined. Resonant helical windings have been used to generate helical fields and to control the macroscopic instabilities.

Helical winding current thresholds for plasma disruptions caused by the superposition of magnetic islands with different helicities were theoretically estimated and compared with the experimental values. Satellite islands due to toroidal effects have also been considered.

To investigate the influence of the toroidal effects on the scalar potential due to a toroidal helical current, the exact solution of Laplace's equation was written as a sum of an infinite series of functions. Each partial sum represents the potential within some accuracy.

ACKNOWLEDGMENTS

The authors would like to thank Miss Izabel T. Yokomizo for typing the manuscript.

REFERENCES

- [1] Pulsator Team, Nuclear Fusion 25, 1059 (1985).
- [2] Robinson, D.C., Nuclear Fusion 25, 1101 (1985).
- [3] Huo, Y., Nuclear Fusion 25, 1023 (1985).
- [4] Fagundes, A.N.; Cruz Jr., D.F.; Galvão, R.M.O.; Iraburu, J.E.; Nascimento, I.C.; Sá, W.; Silva, R.P.; Tuszal, A.G.; Vannucci, A. and Vuolo, J.H., "TBR-1 (Brazilian Tokamak)-Recent Results", in these Proceedings.
- [5] Tan, I.H.; Caldas, I.L.; Nascimento, I.C.; Da Silva, R.P.; Sanada, E.K. and Bruha, R., IEEE Trans. on Plasma Science PS-14, 279 (1985).
- [6] Vannuci, A., "Instabilidades de Disruptura no TBR-1", Ph.D. thesis, Physics Institute, University of São Paulo, to be submitted.
- [7] Ueta, A.Y., "Campo Vertical de Equilíbrio no Tokamak TBR-1", M.Sc. thesis, Physics Institute, University of São Paulo (1985).
- [8] Conde, M.E.; Galvão, R.M.O.; Nascimento, I.C.; Sanada, E.K. and Tuszal, A.G., Revista Brasileira de Física 17, 109 (1987).
- [9] Bender, O.W.; Caldas, I.L.; Tan, I.H.; Nascimento, I.C. and Sanada, E.K., "Resonant Helical Windings in TBR-1", Proc. V Japan-Brazil Symposium on Science and Technology (Tokio, 1986), p. 171 (1986).
- [10] Kim, S.B.; Kochanski, T.F. and Snipes, J.A., "A Study of MHD Oscillations in TEXT using Magnetic and Soft X-Ray Diagnostics", Report FRCR #256 (1984).
- [11] Chirikov, B.V., Phys. Reports 52, 263 (1979).
- [12] Morozov, A.I. and Solov'ev, L.S., Rev. Plasma Physics, vol. 2, Consultants Bureau Press, New York (1966).
- [13] Fernandes, A.S.; Heller, M.V.A.P. and Caldas, I.L., "Resonant Helical Windings in Tokamaks", Proc. 13th Eur. Conf. Contr. Fusion and Plasma Heating (Schliersee, 1986), 1986.
- [14] Kucinski, M.Y. and Caldas, I.L., "Toroidal Helical Fields", Proc. 14th Eur. Conf. Contr. Fusion and Plasma Heating (Madrid, 1987), 1987. Kucinski, M.Y. and Caldas, I.L., to be published in Zeit. Naturforschung (1987).
- [15] La Haye, R.J.; Yamagishi, T.; Schaffer, M.S. and Bard, W.D., Nuclear Fusion 21, 1235 (1981).
- [16] Sometani, T. and Yanagibashi, K., Plasma Physics 25, 33 (1983).

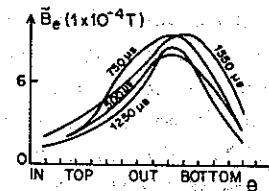


Fig. 1. Oscillation amplitudes \tilde{B}_0 as a function of their angular position θ taken at different times. (Reprinted from Ref. 5).

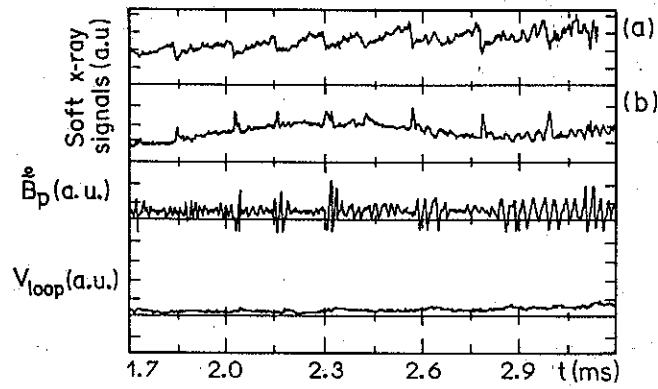


Fig. 2. Temporal evolution, on an expanded timescale, of the soft x-rays signals from the central (a) and the external part (b) of the plasma column, Mirnov oscillation and loop voltage (V_{loop}) during a discharge in TBR-1.

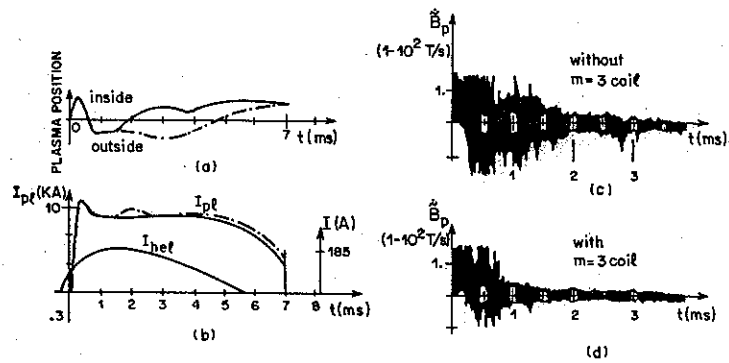


Fig. 3. Displacement of the plasma column (a), temporal profiles of the plasma current with (—) and without (---) $m=3$ coil activation, and MHD activity in these discharges (c and d). (Reprinted from Ref. 9).

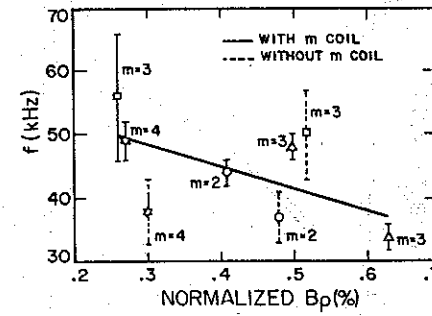


Fig. 4. Dependence of the frequency with the Mirnov oscillation amplitude. (Reprinted from Ref. 9).

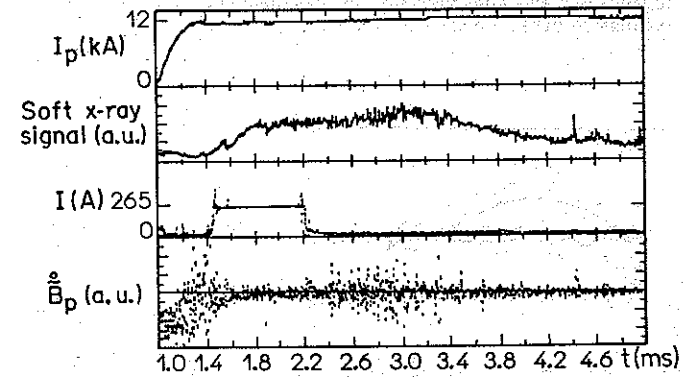


Fig. 5. Temporal evolution of the plasma current (I_p), soft x-rays from the central part of the plasma column, $m=2$ helical winding current (I) and MHD activity during a discharge in TBR-1.

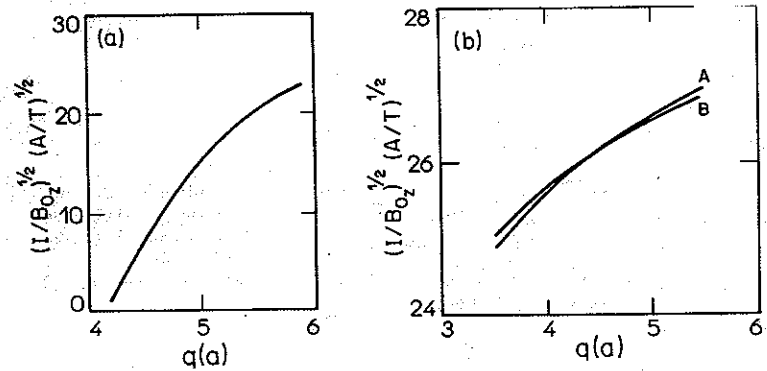


Fig. 6. a) Helical current for overlap of $m=3$ induced and $m=2$ islands in the TBR-1. b) $m=2$ helical current for overlap of $m=2$ and $m=3$ satellite resonances. A and B were obtained neglecting and considering the r -dependence of ψ over the islands width. $q(0) = 1$, $I_p = 10$ kA, $n = 1$.

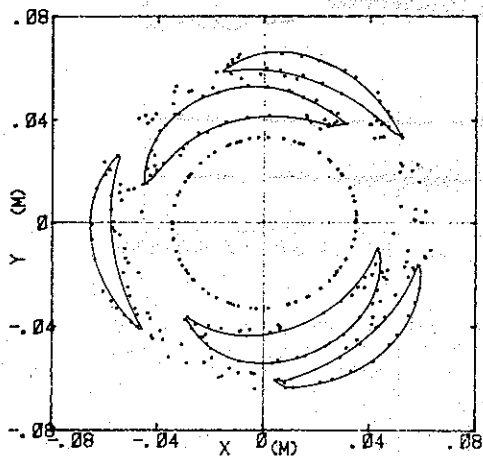


Fig. 7. Intersections of magnetic field lines with the $\phi = 0$ surface for $\bar{B}_g/B_g \approx 0.5\%$, $I = 100$ A, $q(a) = 5$ and $q(0) = 1$.